ENGINEERING COMPUTATIONS, VOL. 12, 641–656 (1995)

NUMERICAL MODELLING AND SIMULATION OF FRICTIONAL CONTACT USING A GENERALISED COULOMB LAW

ANDREAS HEEGE*, PIERRE ALART‡ AND EUGENIO OÑATE†

*Samtech S.A., Liege, Belgium
†International Center for Numerical Methods in Engineering, Barcelona, Spain
‡LMGC, Université Montpellier II, France

ABSTRACT

A consistent formulation for unilateral contact problems including frictional work hardening or softening is proposed. The approach is based on an augmented Lagrangian approach coupled to an implicit quasi-static Finite Element Method. Analogous to classical work hardening theory in elasto-plasticity, the frictional work is chosen as the internal variable for formulating the evolution of the friction convex. In order to facilitate the implementation of a wide range of phenomenological models, the friction coefficient is defined in a parametrised form in terms of Bernstein polynomials. Numerical simulation of a 3D deep-drawing operation demonstrates the performance of the methods for predicting frictional contact phenomena in the case of large sliding paths including high curvatures.

KEY WORDS Curved unilateral contact Frictional work hardening/softening Augmented Lagrangian

INTRODUCTION

In spite of recent advances in the field of computational contact mechanics, most applications reported in the literature are still restricted to Coulomb's law of perfect friction (constant friction coefficient over the entire process). It is well known that such a simplified theory may represent only a limited range of tribological situations[1–4]. The state conditions of surfaces in contact and consequently the friction behaviour, are influenced by a number of complex phenomena related to wear such as chemical reactions, abrasion of coatings etc.[5–8]. Especially for configurations involving large sliding paths, or many repetitions of the same process which is typical for many metal forming operations, the evolution of surface characteristics may become particularly important in the definition of the friction behaviour.

This paper constitutes an attempt to reduce the gap between computational modelling of complex frictional contact problems and physical evidence in practice. Coulomb's law is implemented in a generalised form in order to take into account the evolution of the friction convex as a function of relevant internal variables. To keep the mathematical model general and numerically robust, the friction coefficient is defined in a parametrised form using as polynomial basis Bernstein functions of arbitrary degree[9–11]. In a first approach, the influence of thermal and chemical effects on the evolution of surface characteristics is neglected and the main assumption is that only the frictional work dissipated at the interface between workpiece and tools constitutes the internal variable for the evolution of the friction behaviour.

Within the last few years, one of the most popular approaches for solving frictional contact problems was the augmented Lagrangian method, initially introduced by Hestenes[12] and Powell[13] for non-linear programming problems with equality constraints. It was extended to treat convex

0264–4401/95/070641–16$2.00

Received May 1994
Revised August 1994

differentiable optimisation problems with inequality constraints like the frictionless contact problem by Rockafellar[14]. Lately, within the context of Finite Element Methods, augmented Lagrangian approaches have been successfully applied to frictionless[15,16] and frictional contact problems[17–23]. Coupling the augmented Lagrangian approach and the Finite Element Method yields a mixed formulation where the kinetic variables and the static ones (frictional contact forces) are the final unknowns of the problem. In this paper a Newton-like-iteration for static and kinematic variables is performed and the solution of the unilateral contact problem and the friction problem is obtained simultaneously.

The description is given in the following manner. A contact mechanics summary provides the necessary background and motivation. Although being essentially a review of classical contact and friction laws using the formalism of Convex Analysis[24], this summary conveniently provides a foundation for the generalisation of Coulomb's classical law in order to take into account frictional work hardening/softening. The derivation of a frictional contact operator based on an augmented Lagrangian approach where special attention is paid to take into account the curvature of the contact surface is also discussed briefly. The performance of the method is demonstrated on the example of a deep-drawing simulation of a square cup. The frictional work dissipated in the interface between forming tools and metal sheet, as well as the variation of the friction coefficient, are presented.

CONTACT MECHANICS BACKGROUND

In the following we restrict our attention to the problem of finite deformation of a discretized body of the boundary Γ^{def} which is constrained by the presence of a rigid, instationary obstacle.

Kinematics of curved contact

We note $\vec{x}$ the current position of node of Γ^{def} with respect to a global cartesian reference system. Using an updated Lagrangian formulation, the current position $\vec{x}(\vec{u})$ is defined by an initial position $\vec{X}$, being the equilibrium position of the prior load step and the corresponding displacement vector $\vec{u}$, such that: $\vec{x}(\vec{u}) = \vec{X} + \vec{u}$.

To define the relative displacement of the bodies, it is convenient to take the rigid obstacle for reference and to describe the relative motion of the deformable body with respect to it (see *Figure 1*).

The potential contact surface can be identified with the boundary of the deformable body

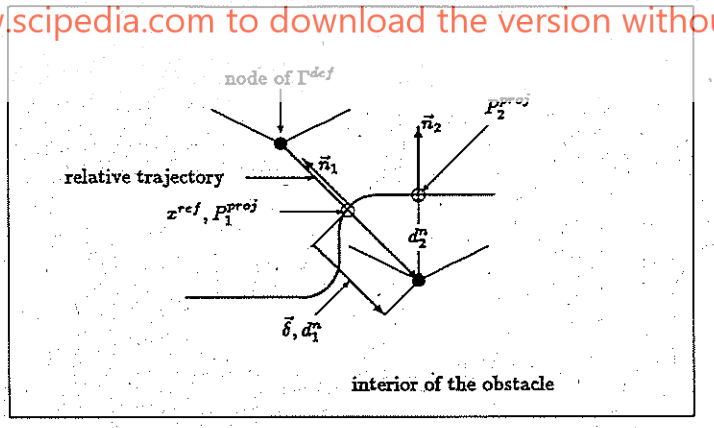

Figure 1 Local contact kinematics—multiple solution of projection: $(P_1^{proj}, \vec{n}_1)$, $(P_2^{proj}, \vec{n}_2)$

Γ^{def} (or a part of it) and is described with reference to a local frame on the boundary of the rigid obstacle Γ^{rig}. In classical approaches the kinematics, as well as the contact and friction laws, are written with respect to a fixed local frame, evaluated currently by the orthogonal projection of $\vec{x}$ on Γ^{rig} at the beginning of each step. This is straightforward for flat contact problems, but in the case of curved contact, particularly if large slip increments occur, this strategy is not efficient.

In this paper, the local frame defined by the outward unit normal vector $\vec{n}(\vec{u})$ to Γ^{rig}, is considered to be unknown at the beginning of each load step, thus varying within the iterative solution of the equilibrium equations due to the curvature of Γ^{rig}.

Normal distance

An appropriate expression for the *signed normal distance* d^n between a node and the obstacle requires the calculus of an implicit local reference position $\vec{P}^{proj}(\vec{u})$ on the obstacle. This reference position is defined by the orthogonal projection of the *current position* of $\vec{x}(\vec{u})$ on Γ^{rig}, thus changing during the equilibrium iterations:

$$\forall \vec{x}(\vec{u}) \in \Gamma^{def}, \qquad \vec{P}^{proj}(\vec{u}) \in argmin[|\vec{z} - \vec{x}|, \qquad \vec{z} \in \Gamma^{rig}] \tag{1}$$

The local frame and specially $\vec{n}(\vec{u})$ associated to each node, is evaluated in $\vec{P}^{proj}(\vec{u})$, yielding the following definition of the signed normal distance:

$$\forall \vec{x}(\vec{u}) \in \Gamma^{def}, \qquad d^n(\vec{u}) = \vec{n}^T(\vec{u}) \cdot [\vec{x}(\vec{u}) - \vec{P}^{proj}(\vec{u})] \tag{2}$$

In the case where Γ^{rig} is defined by polynomials (for example Bézier surface patches[25–27]), numerical methods have to be used to compute the orthogonal projection defined by (1) and its associated normal vector[21,23].

Tangential slip increment

In order to evaluate the relative tangential velocity $\vec{\delta}^t$ between a node of Γ^{def} and the rigid obstacle, first a reference position $\vec{x}^{ref}$ on Γ^{rig} has to be computed.

It is emphasized that a reference position is associated to each node of Γ^{def} whether the node is in contact with Γ^{rig} or not. In spite of the contact status independent definition of $\vec{P}^{proj}(\vec{u})$ involved in that of the normal distance d^n (Cf. (2)), an appropriate definition of $\vec{x}^{ref}$ for the calculus of $\vec{\delta}^t$ depends on the prior contact status (gap, contact).

In the case that a node was in contact at the solution of the prior time step, the reference position can be determined exactly because it can be derived from the last equilibrium position, such that: $\vec{x}^{ref}(\vec{u}) = \vec{X} + \Delta\vec{U}$ where $\Delta\vec{U}$ is the displacement increment of the obstacle.

In the case that a node is in contact during the actual time step, the calculation of the impact-reference position is less trivial and mainly two procedures are used: either a projection of $\vec{X}$ on Γ^{rig} or an impact search strategy. The reference position by projection is obtained by solving (1) where $\vec{x}(\vec{u})$ is replaced by $\vec{X}$. As depicted in *Figure 1*, the solution of problem (1) is generally not unique, (that is why the symbol $\in$ in (1)) requires additional criteria to select a proper solution. In the case that there exist multiple solutions on different surfaces (for example different patches of a CAGD-model[9,10], procedures to select a proper solution can be found in[16,21]. In the case that there are several solutions on one surface patch, the uniqueness of the projection might be obtained by the concept of focal point locus[28]. Referring to the particular kinematical configuration shown in *Figure 1*, the solution of the impact search strategy (i.e. $\vec{x}^{ref}$) which is based on the relative displacement between $\vec{x}$ and Γ^{rig} would be unique. However, it should be mentioned that the a priori more precise impact search strategy is numerically less robust than the projection and yields only a solution, if the relative displacement in between $\vec{x}$ and Γ^{rig} is nonzero (for more details see References 21, 23).

In the case of an incremental solution of quasi-static field problems, the relative tangential velocity $\vec{\delta}^t$, involved in the formulation of the friction law, can be replaced directly by the

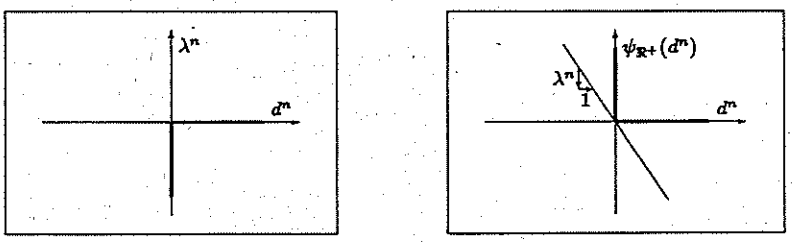

Figure 2 Unilateral contact law—Contact pressure inclusion λ^n

corresponding slip increment $\vec{\delta}^t = \dot{\vec{\delta}}^t \Delta t$. Using again the outward normal $\vec{n}(\vec{u})$ in $\vec{P}^{proj}(\vec{u}) \in \Gamma^{rig}$ the tangential component of the relative displacement increment can be written as*:

$$\vec{\delta}^t(\vec{u}) = (\mathbf{I} - \vec{n}(\vec{u})\vec{n}^T(\vec{u}))\vec{\delta} = (\mathbf{I} - \vec{n}(\vec{u})\vec{n}^T(\vec{u}))(\vec{x}(\vec{u}) - \vec{x}^{ref}) \tag{3}$$

Contact and friction laws

For measuring the relative motion of two bodies candidate to contact, kinematic variables have been introduced. Interaction of the bodies is enforced by the corresponding static variables, i.e. frictional contact forces after discretization. It is convenient to resolve the contact force $\vec{\lambda}$ into normal and tangential components:

$$\vec{\lambda} = \lambda^n \vec{n} + \vec{\lambda}^t \tag{4}$$

In the following, we formulate the normal contact law and proceed with the frictional contact law.

Unilateral contact law

Usually, two exclusive contact status: gap ($d^n > 0$, $\lambda^n = 0$) or contact ($d^n = 0$, $\lambda^n < 0$) are classically formulated by an impenetrability condition, a compression condition and a complementarity condition:

$$d^n \geqslant 0, \qquad \lambda^n \leqslant 0, \qquad \lambda^n d^n = 0 \tag{5}$$

The multivalued contact law $\lambda^n(d^n)$ and its inverse $d^n(\lambda^n)$ can be shown to derive from two conjugate pseudo- (i.e. non-differentiable) potentials, in the form of two similar inclusions:

$$\lambda^n \in \partial\psi_{\mathbb{R}^+}(d^n) \qquad \text{or} \qquad d^n \in \partial\psi_{\mathbb{R}^-}(\lambda^n) \tag{6}$$

where $\psi_{\mathbb{R}^+}$ is the indicator function of the positive half line, $\partial\psi_{\mathbb{R}^+}$ its sub-differential and $\psi_{\mathbb{R}^-}$ its conjugate[24].

Law of contact with perfect friction

Coulomb's classical law states that two bodies in steady contact either stick to each other or they slip on each other along a same direction. These two exclusive status are traditionally expressed by a slip rule, friction criterion and a complementarity condition:

$$\dot{\vec{\delta}}^t = |\dot{\delta}^t| \frac{\vec{\lambda}^t}{|\lambda^t|} \text{ (slip rule)}$$

$$|\lambda^t| \leqslant -\mu\lambda^n \text{ (friction criterium)}$$

$$|\dot{\delta}^t|(|\lambda^t| + \mu\lambda^n) = 0 \text{ (complementarity condition)} \tag{7}$$

*I designates the identity tensor of second order

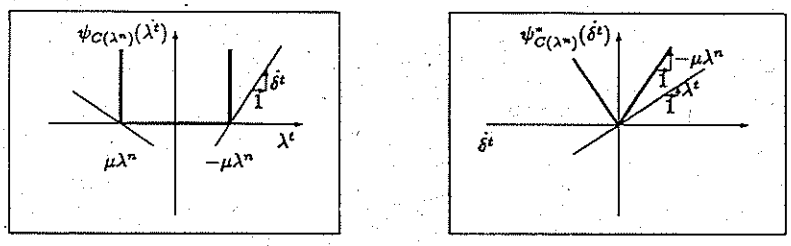

Figure 3 Slip rate inclusion $\dot{\delta}^t$—Friction shear inclusion λ^t

where the friction coefficient μ, still is assumed to be constant. As for unilateral contact, the multivalued slip law $\dot{\vec{\delta}}^t(\vec{\lambda}^t)$ and its inverse, the multivalued friction law $\vec{\lambda}^t(\dot{\vec{\delta}}^t)$, can both be shown to derive from two conjugate pseudo-potentials, in the form of two different inclusions (see *Figure 3*):

$$\dot{\vec{\delta}}^t \in \partial\psi_{C(\lambda^n)}(\vec{\lambda}^t) \quad \text{or} \quad \vec{\lambda}^t \in \partial\psi^*_{C(\lambda^n)}(\dot{\vec{\delta}}^t), \qquad \lambda^n \leqslant 0$$

where

$$C(\lambda^n) = \{\vec{\lambda}^t / |\vec{\lambda}^t| + \mu\lambda^n \leqslant 0\} \tag{8}$$

It should be noted that in quasi-static cases, the slip rate $\dot{\vec{\delta}}^t$ must be approximated by slip increments $\vec{\delta}^t$. Due to the homogeneity of the normal cone $\partial\psi_{C(\lambda^n)}$, this operation simply consists in replacing in expression (8) the slip rate $\dot{\vec{\delta}}^t$ by the increment $\vec{\delta}^t$.

According to Coulomb's classical law, the friction shear is proportional to the contact pressure. Unfortunately, this coupling is not symmetric: the contact pressure is independent of the friction shear but the friction criterium depends on the contact pressure.

Generalised law of frictional contact with hardening/softening

In the following Coulomb's classical law is generalised in order to formulate the evolution of the friction convex as a function of some internal variables. Disregarding anisotropic friction[29,30], only the friction criterion and the complementary condition have to be rewritten in a more general form:

$$|\lambda^t| \leqslant -\mu(\theta)\lambda^n \text{ (generalised friction criterium)}$$

$$|\dot{\delta}^t|(|\lambda^t| + \mu(\theta)\lambda^n) = 0 \text{ (generalised complementarity condition)} \tag{9}$$

where $\mu(\theta)$ presents now the generalised friction coefficient which is assumed to be a function of the single parameter θ. This parameter might be a function of different state variables like for example the relative sliding velocity or the temperature, as well as a function of internal variables like the cumulated slip or the frictional work.

Analogous to classical isotropic work hardening theory in plasticity, it is assumed that the frictional work constitutes the internal variable for formulating the evolution of the friction coefficient. Taking into account that the numerical analysis of a metal forming operation requires an incremental approximation of the process, the frictional work associated to a node of Γ^{def} is obtained by summing up the integrals with respect to each load step interval Δt. Thus, the increment of the frictional work $\Delta\Psi(t)$ is computed by integrating the frictional contact forces over the sliding path $\vec{s}(\vec{u}(t))$:

$$\Delta\Psi(\vec{u}(t+\Delta t), \vec{\lambda}(t+\Delta t)) = \int_t^{t+\Delta t} \vec{\lambda}(t) \cdot \vec{s}(\vec{u}(t))\mathrm{d}t \tag{10}$$

and the actual frictional work at time $t+\Delta t$ of a node of Γ^{def} is defined by:

$$\Psi(\vec{u}(t+\Delta t),\vec{\lambda}(t+\Delta t)) = \Psi(\vec{u}(t),\vec{\lambda}(t)) + \Delta\Psi(\vec{u}(t+\Delta t),\vec{\lambda}(t+\Delta t)) \tag{11}$$

Anticipating that the variation of the friction coefficient within one load step is relatively small, its value can be updated in an explitic manner and in this case $\vec{s}(\vec{u}(t))$ in (10) can be replaced by the slip increment $\vec{\delta}^t$. Thus, at convergence of each increment, the computed frictional work of each contact node constitutes the internal variable for formulating the evolution of the associated friction convex $C(\Psi(t),\vec{u}(t),\vec{\lambda}(t))$. Taking into account that $\Psi(\vec{u}(t),\vec{\lambda}(t))$ is formulated in terms of the mixed solution $(\vec{u}(t)),\lambda(t))$, each contact node is endowed with an independent evolutive friction convex. By adopting an evolutive generalised Coulomb law, the frictional work $\Psi(\vec{u}(t),\vec{\lambda}(t))$ at time t becomes the internal variable for the definition of the friction coefficient $\mu(\Psi(\vec{u}(t),\lambda(t))) = \mu(\theta[\Psi(\vec{u}(t),\vec{\lambda}(t))])$.

In the following we will formulate the friction coefficient by a parametrised polynomial curve using as polynomial base Bernstein functions of arbitrary degree m[9–11]. Adopting as polynomial base Bernstein functions has the advantage that also higher order curves can be constructed with only one curve segment with less tendency to introduce oscillations like for example Lagrange polynomials. The parameter $\theta(t)$ of the polynomial curve is defined by:

$$\theta(\vec{u}(t),\vec{\lambda}(t)) = \frac{\Psi(\vec{u}(t),\vec{\lambda}(t))}{\bar{\Psi}|^{\mu|_{cut}}_{max}} \qquad for \qquad \Psi(\vec{u}(t),\vec{\lambda}(t)) \leqslant \bar{\Psi}|^{\mu|_{cut}}_{max}$$

$$\theta(\vec{u}(t),\vec{\lambda}(t)) = 1 \qquad for \qquad \Psi(\vec{u}(t),\vec{\lambda}(t)) > \bar{\Psi}|^{\mu|_{cut}}_{max} \tag{12}$$

where $\bar{\Psi}|^{\mu|_{cut}}_{max}$ can be interpreted as a threshold in order to take into account that the friction coefficient approaches after preliminary work hardening/softening a constant value for the case that the frictional work exceeds a certain limit. From a practical point of view, this particularity of the mathematical formulation is well suited for the phenomenological modelling of processes where running in effects have to be taken into account in the friction behaviour. Accordingly $\mu|_{cut}$ presents a cut off value for the friction coefficient which is imposed if the frictional work exceeds $\bar{\Psi}|^{\mu|_{cut}}_{max}$. Thus the evolutive friction coefficient is defined as:

$$\mu[\theta(\Psi(\vec{u}(t),\vec{\lambda}(t)))] = \sum_{i=0}^{m} B_{i,m}(\theta) P_i \qquad with \qquad \theta \in [0,1] \tag{13}$$

where $B_{i,m}(\theta)$ is the i^{th} Bernstein function of degree m:

$$B_{i,m}(\theta) = C_m^i \theta^i (1-\theta)^{m-i} \qquad with \qquad C_m^i = \frac{m!}{i!(m-i)!} \tag{14}$$

and the polynomial coefficients P_i define the work hardening/softening of the friction convex. Taking advantage of the properties of a curve which is defined by Bernstein functions, a physical meaning can be associated to the coefficients P_0 and P_m.

For a particle (or node after Finite Element discretization) which has suffered no frictional work, we can derive from (12) and (13):

$$\mu(\theta=0) = \mu|_{init} = \sum_{i=0}^{m} B_{i,m}(0) P_i \equiv P_0 \tag{15}$$

and analogously for a particle where the frictional work exceeds the threshold $\bar{\Psi}|^{\mu|_{cut}}_{max}$:

$$\mu(\theta=1) = \mu|_{cut} = \sum_{i=0}^{m} B_{i,m}(1) P_i \equiv P_m \tag{16}$$

Thus P_0 is identified as the classical friction coefficient of Coulomb's law without friction hardening and the coefficient P_m is the friction coefficient corresponding to the cut off value

$\mu|_{cut}$. The remaining coeffients P_i for $i=1, \ldots, (m-1)$ define the shape of the friction hardening curve as a function of the frictional work.

From a practical point of view, the polynomial curve defined in (13) enable to present a wide range of phenomenological models, but unfortunately there is still a lack of experimental data in order to identify the coefficients P_i.

MIXED FORMULATION FOR CURVED CONTACT

For a complete formulation of the frictional contact problem, the differential inclusions (6) and (8) have to be added to the equilibrium equations of the deformable body. Assuming formally the existence of a differentiable total energy functional $\Phi(\vec{v})$ for characterizing the elastic response of the deformable body, as well as the external forces, coulping contact and friction reduces to adding the two corresponding pseudo-potentials to the potential $\Phi(\vec{v})$:

$$\vec{u} = argmin\{\Phi(\vec{v}) + \psi_{\Re+}[d^n(\vec{v})] + \psi^*_{C(\vec{u})}[\vec{\delta}^t(\vec{u},\vec{v})]\} \tag{17}$$

It is mentioned that (17) states the problem of a single load step of an incremental analysis. It is recalled that the variation of the friction coefficient during one load step is assumed to be so small that it is sufficient to perform after the solution of (17) only an updating of the generalised friction coefficient corresponding to the evolution of the frictional work. Consequently the frictional work does not appear as an extra stored free energy term in (17).

In order to take into account large slips on curved surfaces, the kinematic (contact) variables are written as a function of the virtual displacement $\vec{v}$ and of the solution $\vec{u}$:

$$d^n(\vec{v}) = \vec{n}^T(\vec{P}^{proj}(\vec{v}))\cdot[\vec{x}(\vec{v}) - \vec{P}^{proj}(\vec{v})] \quad \text{and} \quad \vec{\delta}^t(\vec{u},\vec{v}) = (\mathbf{I} - \vec{n}(\vec{u})\vec{n}^T(\vec{u}))(\vec{x}(\vec{v}) - \vec{x}^{ref}) \tag{18}$$

Although the normal distance d^n is a complex function of $\vec{v}$, it can be proved (see Reference 16) that its gradient is equivalent to the normal vector $\vec{n}^T(\vec{P}^{proj}(\vec{v}))$ as for flat contact. Consequently, the system of equations deriving from a quasi-Lagrangian is not modified by the curvature and the expression proposed by Alart & Curnier[17] is recovered.

It is mentioned that, the problem (17) can not be considered as a standard optimisation problem because the objective function depends on the virtual variables $\vec{v}$ and also on the solution $\vec{u}$, because of the dependence of Coulomb's cone $C(\vec{u})$ on the solution $\vec{u}$ through λ^n.

In order to translate expression (17) into a set of equations which are suited for implementation in a computer code, an augmented Lagrangian approach is adopted[12–14]. In the following, only the final expression of the resulting frictional contact operator will be presented and for a theoretical discussion it is referred to[17,21,23].

A couple $(\vec{u},\vec{\lambda})$ is solution of an equilibrium under constraints due to frictional contact, if the following system of equations is satisfied:

$$\begin{Bmatrix} \{\nabla_{\vec{v}}\Phi(\vec{u}) + \mathbf{F}^{equi}(\vec{u},\vec{\lambda})\} \\ \{\mathbf{F}^{suppl.}(\vec{u},\vec{\lambda})\} \end{Bmatrix} = \begin{Bmatrix} \{\vec{0}\} \\ \{\vec{0}\} \end{Bmatrix} \tag{19}$$

From a mechanical point of view, expression (19) presents for each node of Γ^{def} a system of equations with six unknowns (3D) where we can distinguish between kinematic variables ($\vec{u}$-primal) and static variables ($\vec{\lambda}$-dual). Referring to the first line of expression (19) and anticipating that there are no explicitly imposed external forces, $\nabla_{\vec{v}}\Phi(\vec{u})$ presents the internal forces and $\mathbf{F}^{equi}(\vec{u},\vec{\lambda})$ imposes the constraints due to frictional contact. Thus we can interpret the suboperator $\mathbf{F}^{equi}(\vec{u},\vec{\lambda})$ as the 'equilibrium operator', since equilibrium of a node of Γ^{def} can be written as: $\nabla_{\vec{v}}\Phi(\vec{u}) + \mathbf{F}^{equi}(\vec{u},\vec{\lambda}) = \vec{0}$. The function of $\mathbf{F}^{suppl.}(\vec{u},\vec{\lambda})$ is to introduce the additional equations necessary to evaluate the frictional contact forces according to (6,8).

In order to define the explicit expressions of the frictional contact operator, an augmented multiplier for curved applications is introduced:

$$\vec{\sigma}(\vec{u},\vec{\lambda}) = \sigma^n(\vec{u},\vec{\lambda})\vec{n}(\vec{u}) + \vec{\sigma}^t(\vec{u},\vec{\lambda}) = (\lambda^n(\vec{u},\vec{\lambda}) + rd^n(\vec{u}))\vec{n}(\vec{u}) + (\vec{\lambda}^t(\vec{u},\vec{\lambda})) + r\vec{\delta}^t(\vec{u}) = \vec{\lambda} + r(d^n(\vec{u})\vec{n}(\vec{u}) + \vec{\delta}^t(\vec{u})) \tag{20}$$

Remembering that the outward normal $\vec{n}(\vec{u})$ to the obstacle depends on the solution $\vec{u}$, also the decomposition of the frictional contact force $\vec{\lambda}$ into normal and tangential components has to be written as a function of $(\vec{u},\vec{\lambda})$:

$$\lambda^n(\vec{u},\vec{\lambda})=\vec{\lambda}\cdot\vec{n}(\vec{u}) \qquad \textit{and, respectively,} \qquad \vec{\lambda}^t(\vec{u},\vec{\lambda})=\vec{\lambda}-\lambda^n(\vec{u},\vec{\lambda})\vec{n}(\vec{u}) \tag{21}$$

Introducing a projection operator, noted *proj*, the frictional contact operator can be defined:

$$\mathbf{F}^{equi}(\vec{u},\vec{\lambda})=proj_{\mathfrak{R}_-}\{\sigma^n(\vec{u},\vec{\lambda})\}\vec{n}(\vec{u})+proj_{C(proj_{\mathfrak{R}_-}[\sigma^n(\vec{u},\vec{\lambda})])}\{\vec{\sigma}^t(\vec{u},\vec{\lambda})\} \tag{22}$$

and, respectively:

$$\mathbf{F}^{suppl.}(\vec{u},\vec{\lambda})=-\frac{1}{r}[\vec{\lambda}-\mathbf{F}^{equi}(\vec{u},\vec{\lambda})] \tag{23}$$

It is worth-while to mention that the projection operator appearing in (22,23) is due to the inequalities inherent in the contact and friction laws and is necessary for formulating these laws in terms of equations instead of inequalities. A crucial point involved in the derivation of the proposed augmented Lagrangian consists in replacing the classical convex of Coulomb's law $C(\lambda^n)$ by the 'augmented' one $C(proj_{\mathfrak{R}_-}[\sigma^n(\vec{u},\vec{\lambda})])$[17,21,23].

In the following, the contact friction operator corresponding to each contact status is derived from (22) and (23). In classical approaches the contact status is exclusively determined by either kinematic or static variables, whereas the augmented multiplier has the inherent advantage to be a linear combination of both.

Absence of contact is detected if the normal component of the augmented multiplier satisfies $\sigma^n\geqslant 0$, yielding:

$$\text{if } \sigma^n\geqslant 0\Rightarrow\textbf{gap}\Rightarrow\mathbf{F}^*\|_{gap}(\vec{u},\vec{\lambda})=\begin{Bmatrix}\vec{0}\\ -\frac{1}{r}\vec{\lambda}\end{Bmatrix} \tag{24}$$

A sticking node is detected if: $|\vec{\sigma}^t|+\mu(\theta)\sigma^n<0$, and the corresponding sub-operators are evaluated to:

$$\text{if } |\vec{\sigma}^t|+\mu(\theta)\sigma^n<0\Rightarrow\textbf{stick}\Rightarrow\mathbf{F}^*\|_{stick}(\vec{u},\vec{\lambda})=\begin{Bmatrix}\sigma^n(\vec{u},\vec{\lambda})\vec{n}(\vec{u})+\vec{\sigma}^t(\vec{u},\vec{\lambda})\\ d^n(\vec{u})\vec{n}(\vec{u})+\vec{\delta}^t(\vec{u})\end{Bmatrix} \tag{25}$$

Analogously for a sliding node the tangential force has to hold: $|\vec{\sigma}^t|+\mu(\theta)\sigma^n\geqslant 0$ and we can derive from (22) and (23) the corresponding sub-operators:

$$\text{if } |\vec{\sigma}^t|+\mu(\theta)\sigma^n\geqslant 0\Rightarrow\textbf{slip}\Rightarrow\mathbf{F}^*\|_{slip}(\vec{u},\vec{\lambda})=\begin{Bmatrix}\sigma^n(\vec{u},\vec{\lambda})[\vec{n}(\vec{u})-\mu(\theta)\vec{t}(\vec{u},\vec{\lambda})]\\ d^n(\vec{u})\vec{n}(\vec{u})-\frac{1}{r}[\vec{\lambda}^t(\vec{u})+\mu(\theta)\sigma^n(\vec{u},\vec{\lambda})\vec{t}(\vec{u},\vec{\lambda})]\end{Bmatrix} \tag{26}$$

where the tangential slip direction unit vector is defined by:

$$\vec{t}(\vec{u},\vec{\lambda})=\frac{\vec{\sigma}^t(\vec{u},\vec{\lambda})}{|\vec{\sigma}^t(\vec{u},\vec{\lambda})|} \tag{27}$$

Recalling that the coupled equations (19) are in general highly non-linear due to frictional contact, as well as due to the non-linearites resulting from large transformations and material laws, iterative methods have to be resorted in order to attempt a solution. The authors confirm a satisfactory performance of the simultaneous solution of the mixed system (19) by a Newton-like-iteration scheme. In the next section, the corresponding contact Jacobian matrices will be presented.

Jacobian matrices of the contact friction operator for curved contact

In order to preserve quadratic convergence when a Newton type solution scheme is used, contributions of geometric terms arising from the gradient of the unit normal vector at contact

points have to be taken into account. Since the generalised friction coefficient is kept constant over each load step of an incremental analysis, thus being updated only at convergence of the iterative solution of (19), no additional terms have to be taken into account for evaluating the tangent contact operator.

In analogy to the tangent stiffness matrix of a finite element, the elemental contact Jacobian $\mathbf{J}^*(\vec{u},\vec{\lambda})$ is defined by the following operation:

$$\mathbf{J}^*(\vec{u},\vec{\lambda}) = \begin{bmatrix} [\nabla_{\vec{u}}\mathbf{F}^{equi}(\vec{u},\vec{\lambda})] & [\nabla_{\vec{\lambda}}\mathbf{F}^{equi}(\vec{u},\vec{\lambda})] \\ [\nabla_{\vec{u}}\mathbf{F}^{suppl.}(\vec{u},\vec{\lambda})] & [\nabla_{\vec{\lambda}}\mathbf{F}^{suppl.}(\vec{u},\vec{\lambda})] \end{bmatrix} \tag{28}$$

Taking into account (24) we obtain as elementary contribution for a node in gap:

$$\mathbf{J}^{gap} = \begin{bmatrix} [\nabla_{u_j}F_i^{equi}] & [\nabla_{\lambda_j}F_i^{equi}] \\ [\nabla_{u_j}F_i^{suppl.}] & [\nabla_{\lambda_j}F_i^{suppl.}] \end{bmatrix} = \begin{bmatrix} [0_{ij}] & [0_{ij}] \\ [0_{ij}] & [-\frac{1}{r}I_{ij}] \end{bmatrix} \quad i,j=1,2,3 \tag{29}$$

Deriving (25), the elementary contributions for a sticking node are evaluated to:

$$\mathbf{J}^{stick} = \{\nabla_{u_\rho}\nabla_{\lambda_j}\} \begin{Bmatrix} \{\sigma^n(\vec{u},\vec{\lambda})\vec{n}_i(\vec{u}) + \sigma_i^t(\vec{u},\vec{\lambda})\} \\ \{d^n(\vec{u})n_i(\vec{u}) + \delta_i^t(\vec{u})\} \end{Bmatrix} = \begin{bmatrix} [P_{ij}+C_{ij}] & [I_{ij}] \\ [\frac{1}{r}(P_{ij}+C_{ij}^*)] & [0_{ij}] \end{bmatrix} \quad i,j=1,2,3 \tag{30}$$

where the second order tensor P_{ij} presents the contribution which is independent of the curvature:

$$P_{ij} = r[I_{ij} - n_i n_j + n_i \nabla_{u_j} d^n] \tag{31}$$

The contributions due to the curvature of the obstacle are a function of the gradient of the normal to the obstacle $\nabla_{u_j} n_k$:

$$C_{ij} = -r(\delta_k^t + d^n n_k)\nabla_{u_j} n_k n_i \qquad \text{and} \qquad C_{ij}^* = -r(\delta_k^t n_i \nabla_{u_j} n_k + \delta_p n_p \nabla_{u_j} n_i) \tag{32}$$

Recalling that the gradient of the normal distance $\nabla_{u_j} d^n$ is equivalent to the normal n_j at the respective contact point (see also Reference 16) and taking advantage of the fact, that the imposed spatial position of a sticking node is independent of the curvature of the obstacle (for more details see Reference 21), the elemental contribution to the Jacobian matrix of a sticking node can be simplified to:

$$\mathbf{J}^{stick} = \begin{bmatrix} [rI_{ij}] & [I_{ij}] \\ [I_{ij}] & [0_{ij}] \end{bmatrix} \quad i,j=1,2,3 \tag{33}$$

Analogously, the slip Jacobian is evaluated to:

$$\mathbf{J}^{slip} = \begin{bmatrix} [rM_{ij} + N_{ik}\nabla_{u_j} n_k] & [M_{ij}] \\ [M_{ij} + \frac{1}{r}N_{ik}\nabla_{u_j} n_k] & [\frac{1}{r}(M_{ij} - I_{ij})] \end{bmatrix} \quad i,j=1,2,3 \tag{34}$$

The term which is independent of the obstacles curvature is:

$$M_{ij} = [n_i - \mu t_i]\nabla_{u_j} d^n + \rho(I_{ij} - n_i n_j - t_i t_j) \tag{35}$$

The supplementary curvature terms can be identified, since they are coupled to the gradient $\nabla_{u_j} n_k$ (see (34)):

$$N_{ik} = \lambda_k[n_i - \mu t_i] + \sigma^n I_{ik} - \rho[(\lambda_k + r\delta_k)n_i - (\lambda_p + r\delta_p)n_p(t_i t_k - I_{ik})] \tag{36}$$

Since the term $\rho(I_{ij} - n_i n_j - t_i t_j)$ appearing in (35) vanishes for 2D applications, it can be identified as the specific 3D term. We mention that (34) does not depend on the geometrical description of the obstacle. For the particular case that the surface is defined by an implicit function, the term $N_{ik}\nabla_{u_j} n_k$ can be split into an intrinsic curvature term and a coupled 3D-curvature term[21,29,30].

NUMERICAL EXAMPLE

In the following deep-drawing simulation frictional hardening/softening is taken into account, but it is emphasized that the phenomenological model used is not based on experimental data. From a practical point of view, it is very difficult to measure a local variation of the friction coefficient and experimental data suitable to identify the parameters of the proposed generalised Coloumb law is not available yet.

The frictional work hardening/softening curve is defined by a Bernstein polynomial of degree $m=3$ using uniform parametrisation (see (13)). For convenience it is imposed that $P_1 \equiv P_0$ and $P_2 \equiv P_m$. As a consequence of this, the resulting curve has an asymptotic behaviour at both extremes, is antisymmetric with respect the coordinates $(\theta=1/2, \mu=1/2(\mu|_{init}+\mu|_{cut}))$ and is entirely defined by three constants, namely an initial friction coefficient for zero frictional work $\mu(0)=\mu|_{init}$ and a cut off value of the friction coefficient $\mu(1)=\mu|_{cut}$ corresponding to a frictional work of $\bar{\Psi}|_{max}^{\mu|_{cut}}$ (see *Figure 4*).

For discretizing the metal sheet eight node solid finite elements had been used. The formulation is characterized by the following features: updated Lagrangian formulation for small elastic-finite-plastic strains, Hill's orthotropic yield function with isotropic hardening and associated flow rule. In order to avoid locking or hourglassing, a selective reduced integration scheme is used[31,32]. In the following examples, the load step increment is controlled by a R_{min} strategy[31,32] which consists of adapting automatically the step size in such a way that some limitations on the increments of internal variables like stresses or rotations are not violated.

Deep drawing of an aluminium square cup

The following deep-drawing simulation of an aluminium square cup has been proposed as one of the benchmark tests of the NUMISHEET'93 conference[33,34]. The tool dimensions are illustrated in *Figure 5* and a summary of the input data for the numerical simulation is given in *Table 1*.

Taking advantage of two symmetry planes, only a quarter of the sheet is discretized into 625 eight node solid finite elements. The blankholder is controlled by a kinematic schedule instead of a prescribed global force. This implies that the blankholder force which is applied on the sheet results from the unknown equilibrium configuration. The initial position of the blankholder (i.e. for zero punch travel) is such that the space in between die and blankholder is equal to the initial sheet thickness. While the punch is travelling 30 mm downwards, the blankholder is moving 0.5 mm upwards such that the space in between blankholder and die is varying linearly from initially the sheet thickness up to the sheet thickness plus 0.5 mm space at the maximum punch travel.

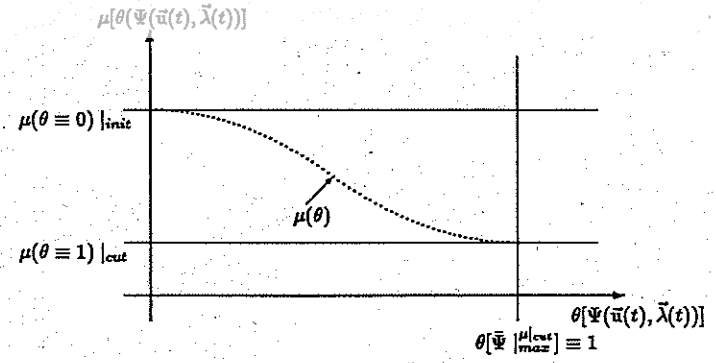

Figure 4 Phenomenological model of frictional contact with hardening

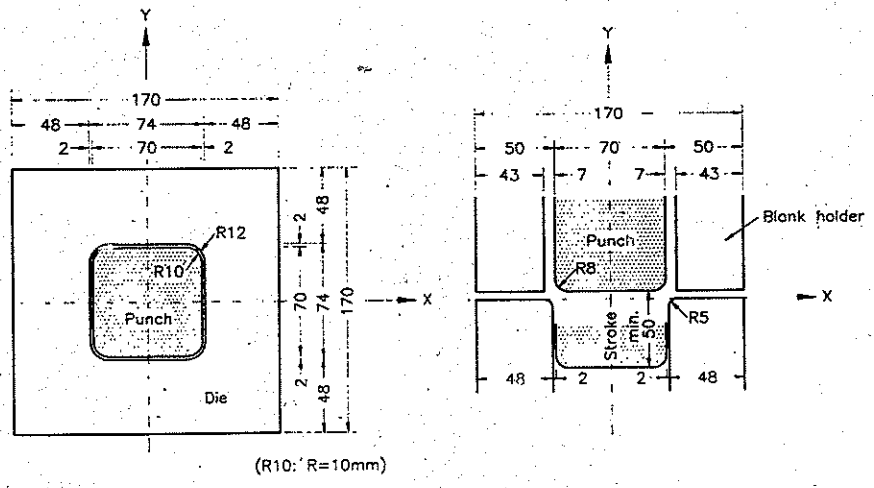

Figure 5 Tool dimensions—deep drawing of a square cup

Table 1 Summary of input data—square cup

Initial sheet geometry:	
width/2	75 mm
length/2	75 mm
thickness	0.81 mm
Formulation:	Updated lagrangian
Constitutive equation	isotropic, elasto-plastic, large transf.
Gauss integration pattern	selective reduced integration ($\bar{B}$)
Material data:	
Young's modulus E, Poisson's ratio ν	$E=71$ GPa, $\nu=0.33$
Consts. of Swifts law, $Y=C(\varepsilon_0+\varepsilon^p)^n$:	$\varepsilon_0=0.01658$, $C=0.576$ GPa, $n=0.36$
Control data of frictional contact:	
Penalty factor	70 Nm
Initial friction coefficient $\mu\|_{init}$	0.16
Cut off friction coefficient $\mu\|_{cut}$	0.01
Cut off frictional work $\Psi\|^{\mu\|cut}_{max}$	2 Nm

For the entire simulation 550 increments have been used corresponding to 30h CPU time on a SilconGraphics/Indigo XS 24 computer.

The *Figures 5* and *7* show the frictional work dissipated in between the forming tools and the deforming blank, each figure for 15 mm and 30 mm punch travel respectively. In particular *Figure 6* shows the frictional work distribution with respect to the outer side of the square cup, i.e. the face which is interacting with the die. Analogously *Figure 7* presents the distribution of the frictional work due to frictional contact of the sheet with the punch and the blank holder (inner side of the square cup). It should be noted that in order to make apparent the profiles of the frictional work, different scaling has been used during postprocessing.

Considering the frictional work distribution of the inner face of the deformed sheet (see *Figure 7*), it can be seen that there are two very small regions where high frictional contact occurs close to the curved corner of the blank holder. It can be stipulated that these regions with high local frictional contact occur because the sheet tends to build up wrinkles which are prevented by the blank holder. Further on it can be concluded that frictional contact in between punch and sheet occurs exclusively at the punch radius.

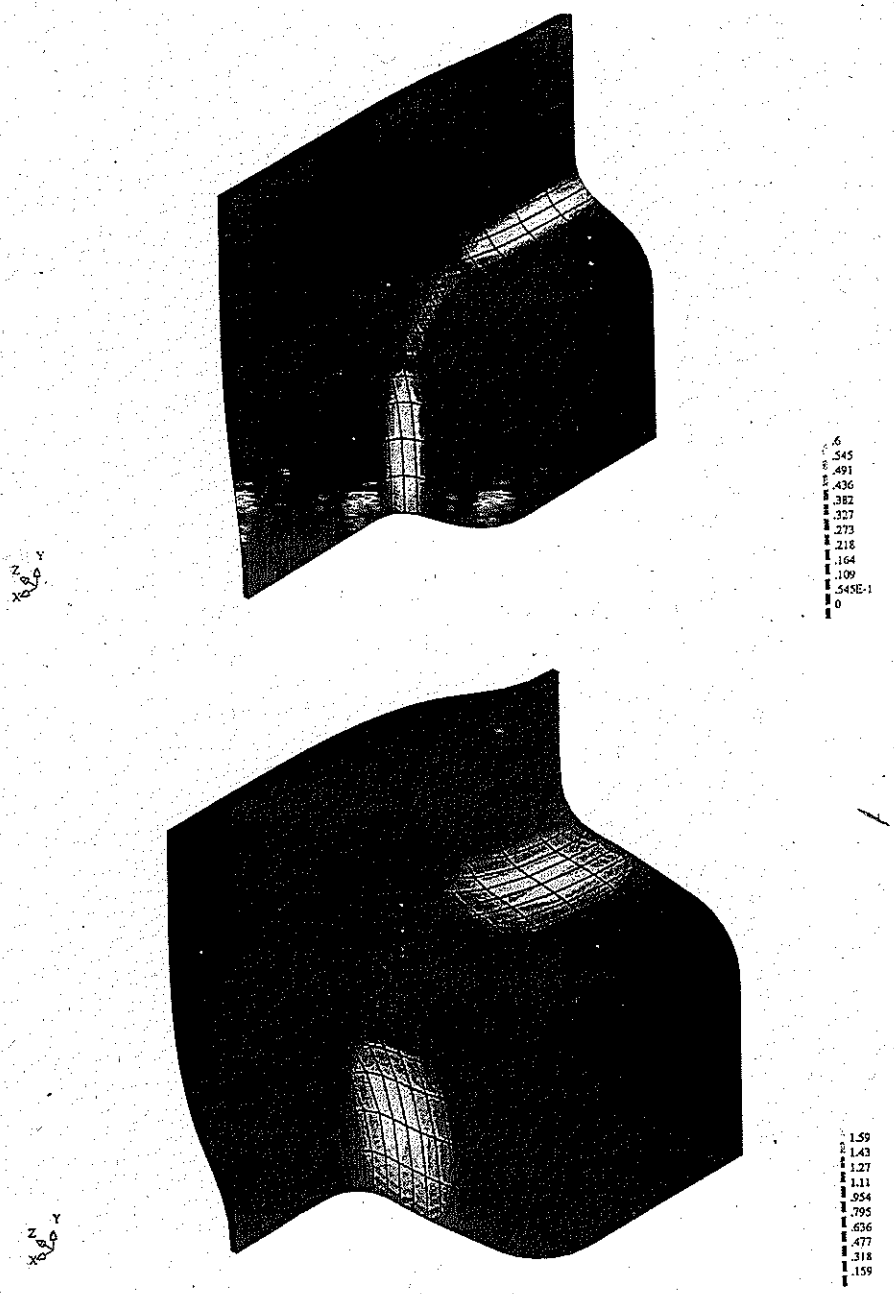

Figure 6 Frictional work after 15 mm and 30 mm punch stroke (in [Nm])—outside of square cup

Comparing the quantitative values of the frictional work distributions of the outer and inner side of the sheet, it is observed that the frictional work dissipated between the die and the sheet is much higher than inside the square cup due to the interaction of the sheet with the punch. Referring to *Figure 6*, it is shown that the highest wear is to be expected at the die radius, in particular at the straight parts of the die radius, i.e. in between the corners of the die.

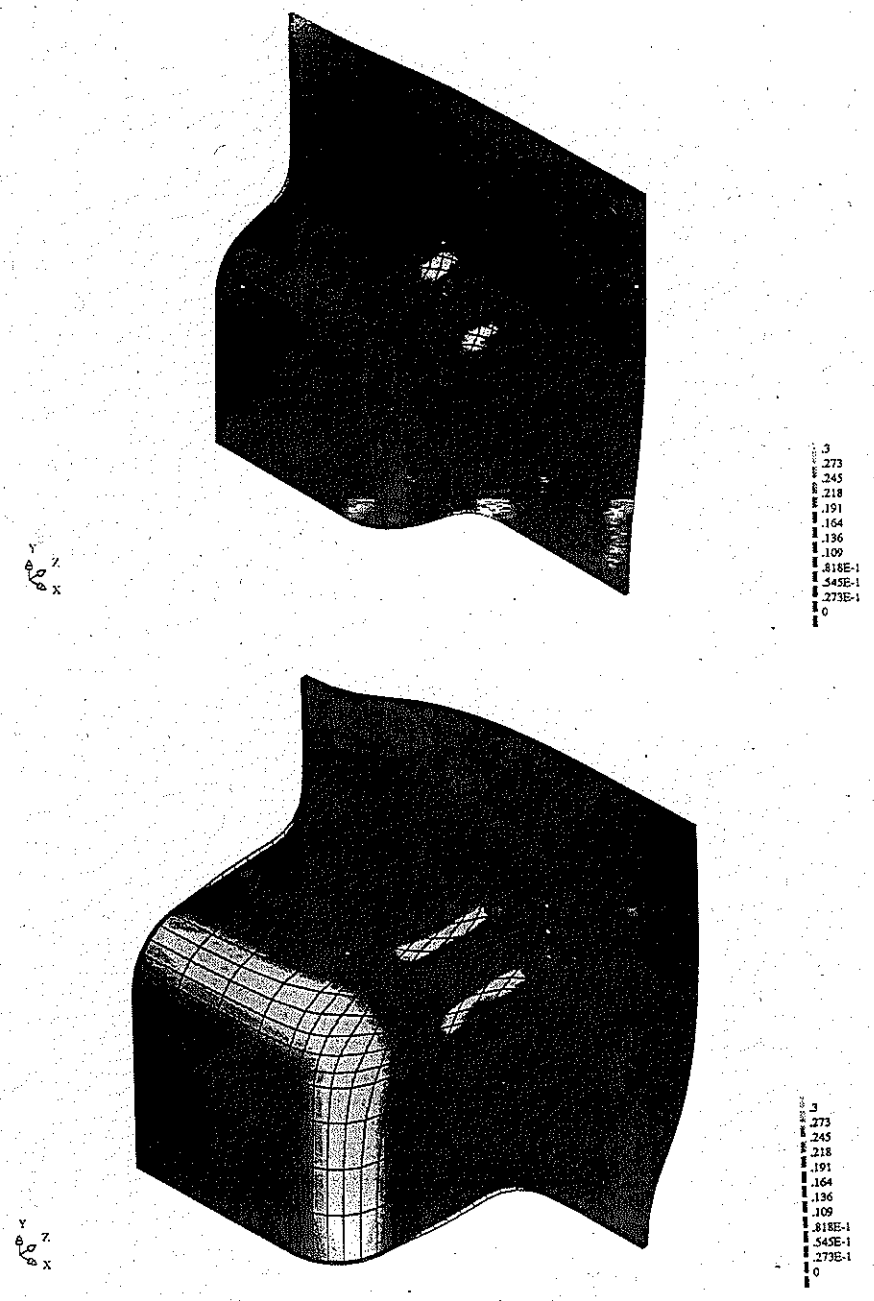

Figure 7 Frictional work after 15 mm and 30 mm punch stroke (in [Nm])—inside of square cup

According to the phenomenological model used to describe the evolution of the friction coefficient, the distribution of the friction coefficient after 15 mm and 30 mm punch travel is shown in *Figure 8*. It can be seen that the distribution of the friction coefficient corresponds to the profile of the frictional work (*Figure 6*).

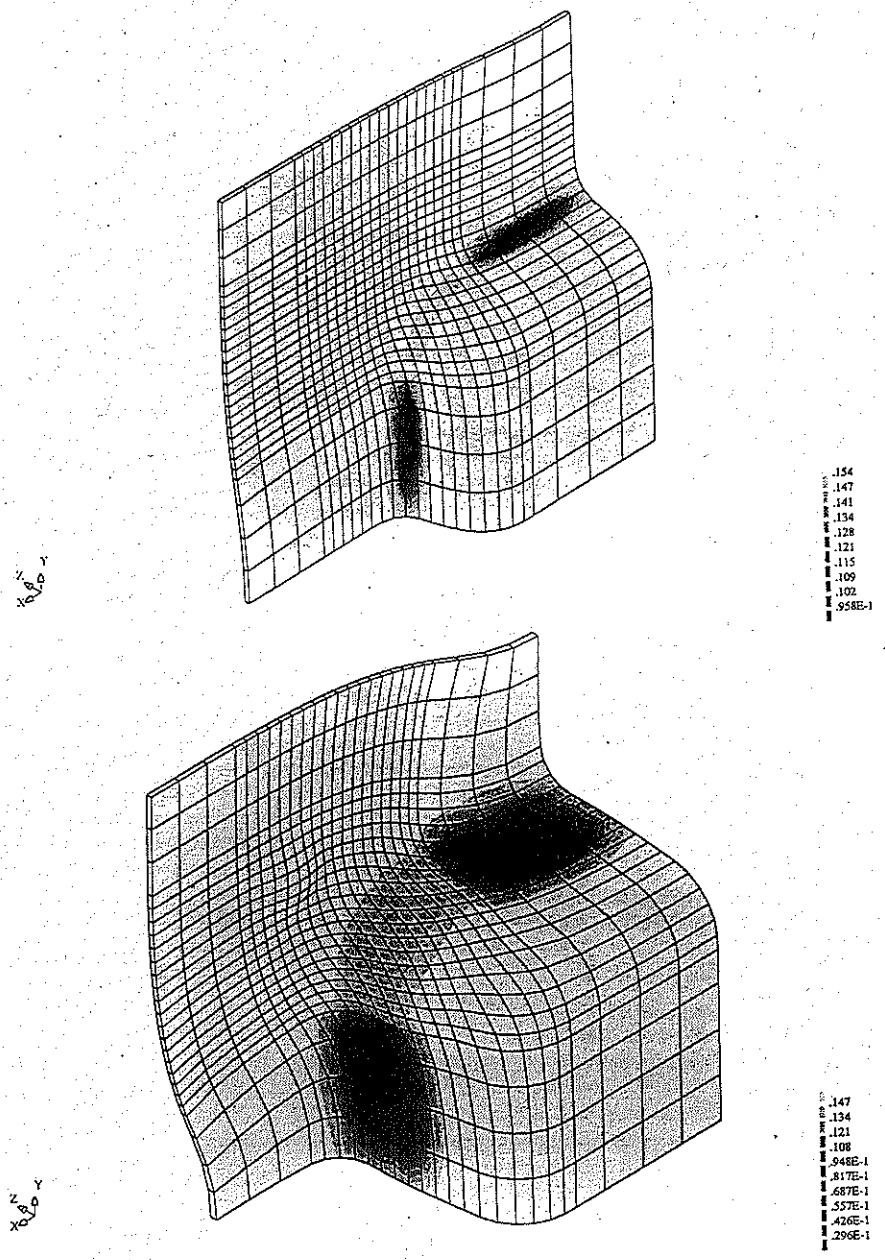

Figure 8 Distribution of friction coefficient after 15 mm and 30 mm punch stroke—outside of square cup

CONCLUDING REMARKS

Inspired from an augmented Lagrangian approach, a mixed formulation for unilateral contact problems including frictional work hardening/softening has been presented.

Analogous to classical work hardening theory in plasticity, it was assumed that the frictional work constitutes the internal variable for the evolution of the generalised Coulomb's cone.

However, any other phenomena which are of importance for the friction behaviour might be included easily in terms of internal variables in the definition of a generalised evolutive friction convex domain. In the proposed mathematical model, the evolution of the friction coefficient was defined by a polynomial curve using Bernstein functions as basis. An advantage of this choice for the polynomial basis is that also curves of relative high order can be constructed by only one curve segment with less tendency to introduce oscillations. Thus friction hardening and/or softening which might be preliminary to running in to a constant value, can be modelled easily without need for fitting different polynomial curve segments.

In spite of the generality of the mathematical formulation, being well suited to take into account a wide range of phenomenological models, the lack of available experimental data is a major obstacle for implementing more advanced realistic frictional contact models.

Using a Newton-like-iteration for kinematic and static variables, the solution of the frictional contact problem is simultaneous. The method has proved to be efficient to handle large slips over curved surfaces even if strong material non-linearities like in the case of elasto-plasticity have to be taken into account. Since the contact algorithm requires no discretization of the contact surfaces, it operates directly on parametric polynomial surface patches or geometrical entities defined by implicit functions, both issued from Computer Aided Geometrical Design. In particular if the contact surfaces involve important curvatures, a discretization of the geometry by linear surfaces has to be avoided. The arguments are that first the number of patches necessary to describe a curved geometry would augment considerably, thus resulting in a higher computational effort for the contact search and secondly, the requirement for smooth surfaces with preferably at least C^1-continuity can not be fulfilled with linear surface patches.

Three-dimensional simulations of metal forming operations have given promising results and it is expected that the application of the presented model, fitted with appropriate experimental data, will improve the quality of numerical simulations.

ACKNOWLEDGEMENTS

The authors are indebted to Christian Teodosiu, director of the laboratory LPTM of the University Paris Nord/France and Luis Menezes, scientist at the University of Coimbra/Portugal, for the development of some of the finite elements used, as well as to the European Community for financial support within the project PREDWEAR—Development of a Decision Support System for Predicting Wear in Bulk and Sheet Forming Operations (Pro. No.: BE-5248-92, Contr. No.: BRE2-CT92-0180).

REFERENCES

1 Avitzur, B. *Handbook of Metal-forming Processes,* John Wiley & Sons, New York, USA (1983)
2 Avitzur, B. *Metal Forming: Processes and Analysis,* McGraw-Hill (1968)
3 Curnier, A. A theory of friction, *Int. J. for Solids and Struct.*, **20**/7, 637–647 (1984)
4 Neto, E. A. de Souza, Hashimoto, K., Peric, Djordje and Owen, D. R. J. A phenomenological model for frictional contact of coated steel sheets, *Proc. NUMISHEET'93,* Isehara/Japan, edt. E. Nakamachi, E. Oñate, R. H. Wagoner, 239–249 (1993)
5 Bowden, F. P. and Tabor, D. *The Friction and Lubrication of Solids,* Clarendon Press, Oxford (1950)
6 Archard, J. P. Friction between metal surfaces, *Wear,* **113**, 3–16 (1986)
7 Wanheim, T. Friction at high normal pressure, *Wear,* **25**, 225–244 (1973)
8 Steffensen, H. and Wanheim, T. Asperities on asperities, *Wear,* **43**, 89–98 (1977)
9 Farin, G. *Curves and Surfaces for Computer Aided Geometrical Design—A Practical Guide,* Harcourt Brace Jovanivocih, Publishers—Academic Press Inc. (1988)
10 Faux, I. D. and Pratt, M. J. *Computational Geometry for Design and Manufacturing,* Ellis Horwood Limited, Chichester/John Wiley & Sons (1979)
11 Bartels, R., Beaty, J. and Barsky, B. *Mathematiques et CAO 6,* HERMES, 75017 PARIS (1987)
12 Hestenes, M. Multiplier and gradient method, *J. Opt. Th. et Appl.*, **4**, 303–320 (1969)
13 Powell, B. T. *A Method for Nonlinear Constraints in Minimisation Problems in Optimisation,* R. Fletcher Edition, Academic Press, London, 283–298 (1969)

14 Rockafellar, R. T. *A Duel Approach to Solving Nonlinear Programming Problems by Unconstrained Optimisation*, **5**, Math. Prog. 5, 354–373 (1973)
15 Wriggers, P., Simo, J. C. and Taylor, R. L. Penalty and augmented lagrangian formulations for contact problems, *Proc.: NUMETA 85 Conf.* (1985)
16 Heegard, J. C. and Curnier, A. An augmented lagrangian method for discrete large slip problems, *Int. J. Num. Meth. in Eng.* **36**, 569–593 (1993)
17 Alart, P. and Curnier, A. A mixed formulation for frictional contact problems prone to newton like solution methods, *Computer Meth. in Appied Mech. and Eng.*, **92**, No. 3, 353–375 (1991)
18 Alart, P. Multiplaceurs augmentés et méthode de newton généralisée pour contact avec frottement, *Document LMA-DME-EPFL Lausanne* (1988)
19 Simo, J. C. and Laursen, T. A. An augmented lagrangean treatment of contact problems involving friction, *Comp. and Struct.*, **42**, 97–115 (1992)
20 De Saxe, G. and Feng, Z. Q. New inequality and functional for contact with friction: the implicit standard material approach, *Mech. Struct. and Mach.*, **19**, 3, 301–325 (1991)
21 Heege, A. *Simulation Numerique 3D du Contact avec Frottement et Application à la Mise en Forme*, PhD thesis, Institut National Polytechnique de Grenoble, France (1992)
22 Heege, A. and Alart, P. On an implicit contact friction algorithm dedicated to 3d sheet forming simulations, *4th Int. Conf. Num. Meth. in Industrial Forming Processes—NUMIFORM'92*, edited by Chenot, J.-L. and Wood, R. D. and Zienkiewicz, O. C., 14–18 September, Valbonne/France, 479–484 (1992)
23 Heege, A. and Alart, P. A frictional contact element for strongly curved contact problems, *Int. J. Num. Meth. in Eng.* (1993)
24 Moreau, J. J. *Application of Convex Analysis to Some Problems of Dry Friction*, **II**, Zorski Ed., Trends of Pure Math. to Mech. 263–280 (1979)
25 Bézier, P. *Mathematical and Practical Possibilities of UNISURF*, Computer-Aided Design, Academic Press, New York (1974)
26 Bézier, P. *Essai de Définition Numérique des Courbes et des Surfaces*, Université Pierre et Marie Curie, PhD Thesis (1977)
27 Bézier, P. *Mathematiques et CAO 4*, HERMES, PARIS (1986)
28 Curnier, A., He, Q.C. and Telega, J. J. Formulation of unilateral contact between two elastic bodies undergoing finite deformations, CRAS, **31**, Serie II No. 2, 1–6 (1992)
29 Alart, P. A simple contact algorithm applied to large sliding and anisotropic friction, *Proc. Contact Mechanics Int. Symp.*, Lausanne, Presses Polytechnique Romandes, 321–336 (1992)
30 Alart, P. and Heege, A. Consistent tangent matrices of curved contact operators involving anisotropic friction, Revue Européenne des Eléments Finis (1994)
31 Menezes, L. F., Teodosiu, C. and Makinouchi, A. 3-d solid elasto-plastic elements for simulating sheet metal forming processes by the finite element method, *FE-Simulation of 3D Sheet Metal Forming Processes in Automotive Industry—Tagungsbericht der VDI-Gesellschaft Fahrzeugtechnik*, **894**, 381–403 (1991)
32 Teodosiu, C., Cao, H. L., Ladreyt, T. and Detraux, J. M. Implicit versus explicit methods in the simulation of sheet metal forming, *FE-Simulation of 3D Sheet Metal Forming Processes in Automotive Industry—Tagungsbericht der VDI-Gesellschaft Fahrzeugtechnik*, **894**, 601–627 (1991)
33 Makinouchi, A., Nakamachi, E., Oñate, E. and Wagoner, R. H., editors. *NUMISHEET'93 2nd Int. Conf.: Num. Simulation of 3-D Sheet Metal Forming Processes—Verification of Simulation with Experiment*, Isehara, Japan, 31 August–2 September (1993)
34 Oñate, E., Garcia Garino, C., Botello, S., Flores, F., Agelet de Saracibar, C., Rojek, J., Oliver, J., Sosnowski, W., Heege, A., Neubert, A. and Ouzunidis, G. Numistamp: A research project for assessment of finite element models for stamping processes, *Proc. of NUMISHEET'93, Isehara/Japan, edt. E. Nakamachi*, E. Oñate, R. H. Wagoner (1993)